International Journal of Nanomedicine

Dovepress
Taylor & Francis Group

Open Access Full Text Article

ORIGINAL RESEARCH

Fusidic Acid and Lidocaine-Loaded Electrospun Nanofibers as a Dressing for Accelerated Healing of Infected Wounds

Khulud A Alsulami[1], Abrar A Bakr[1], Alaa Sirwi[2], Mahmoud A Elfaky[2], Rasheed A Shaik[3], Bayan Y Alshehri[1], Alhassan H Aodah[1], Nojoud Al Fayez[1], Abdullah A Alshehri[1], Fahad A Almughem[1], Abdulrahman A Halwani[4,5], Essam A Tawfik[1]

[1]Advanced Diagnostics and Therapeutics Institute, Health Sector, King Abdulaziz City for Science and Technology (KACST), Riyadh, 11442, Saudi Arabia; [2]Department of Natural Products, Faculty of Pharmacy, King Abdulaziz University, Jeddah, 21589, Saudi Arabia; [3]Department of Pharmacology and Toxicology, Faculty of Pharmacy, King Abdulaziz University, Jeddah, 21589, Saudi Arabia; [4]Department of Pharmaceutics, Faculty of Pharmacy, King Abdulaziz University, Jeddah, 21589, Saudi Arabia; [5]Regenerative Medicine Unit, King Fahad Medical Research Center, King Abdulaziz University, Jeddah, 21589, Saudi Arabia

Correspondence: Essam A Tawfik, Email etawfik@kacst.gov.sa

Introduction: Wound treatment is a significant health burden in any healthcare system, which requires proper management to minimize pain and prevent bacterial infections that can complicate the wound healing process.

Rationale: There is a need to develop innovative therapies to accelerate wound healing cost-effectively. Herein, two polymer-based nanofibrous systems were developed using poly-lactic-co-glycolic-acid (PLGA) and polyvinylpyrrolidone (PVP) loaded with a combination of an antibiotic (Fusidic acid, FA) and a local anesthetic (Lidocaine, LDC) via electrospinning technique for an expedited healing process by preventing bacterial infections while reducing the pain sensation.

Results: The fabricated nanofibers showed an excellent morphology with an average fiber diameter of 556 ± 71 nm and 291 ± 87 nm for the dual drug-loaded PLGA/PVP and PVP nanofibers, respectively. The encapsulation efficiency (EE%) and drug loading (DL) studies revealed that PLGA/PVP loaded with FA and LDC exhibited EE% of 92% and 75%, respectively, while the DL was measured at 40 ± 8 µg/mg for FA and 32 ± 7 µg/mg for LDC. Furthermore, both drugs were fully released from the nanofibers within 48 hours. In contrast, FA/LDC-loaded PVP nanofibers exhibited EE% of 100% for FA and 84% for LDC; DL was measured at 85 ± 3 µg/mg for FA and 70 ± 3 µg/mg for LDC, while both drugs were completely released within 24 hours. The in vitro cytotoxicity study demonstrated a safe concentration of FA and LDC at ≤ 125 µg/mL. The prepared nanofibers were tested in vivo in an *S. aureus*-infected wound mice model to assess their efficacy, and the results showed that the FA/LDC-PVP had a faster wound closure and the lowest bacterial counts compared to other groups.

Conclusion: These findings showed the potential application of the fabricated dual drug-loaded nanofibers as a wound-healing plaster against infected acute wounds.

Keywords: electrospinning, nanofibers, fusidic acid, lidocaine, wound healing, infected wound

Introduction

Skin is the largest organ in the human body, accounting for approximately 10% of an adult's total body weight.[1,2] It acts as a barrier which maintains homeostasis and serves as a defense line against external environmental factors, protecting the internal organs and tissues from physical, chemical, and biological threats. A wound is defined as a disruption of the skin's anatomical structure and function.[3] As the integrity of the skin becomes compromised, due to external forces, disease-related ulceration, or thermal or mechanical damage, the structure and function of the skin will be adversely affected. Therefore, wounds should be appropriately managed to restore the barrier function of the skin, accelerate healing, and prevent further complications.

Received: 1 October 2024
Accepted: 28 December 2024
Published: 20 January 2025

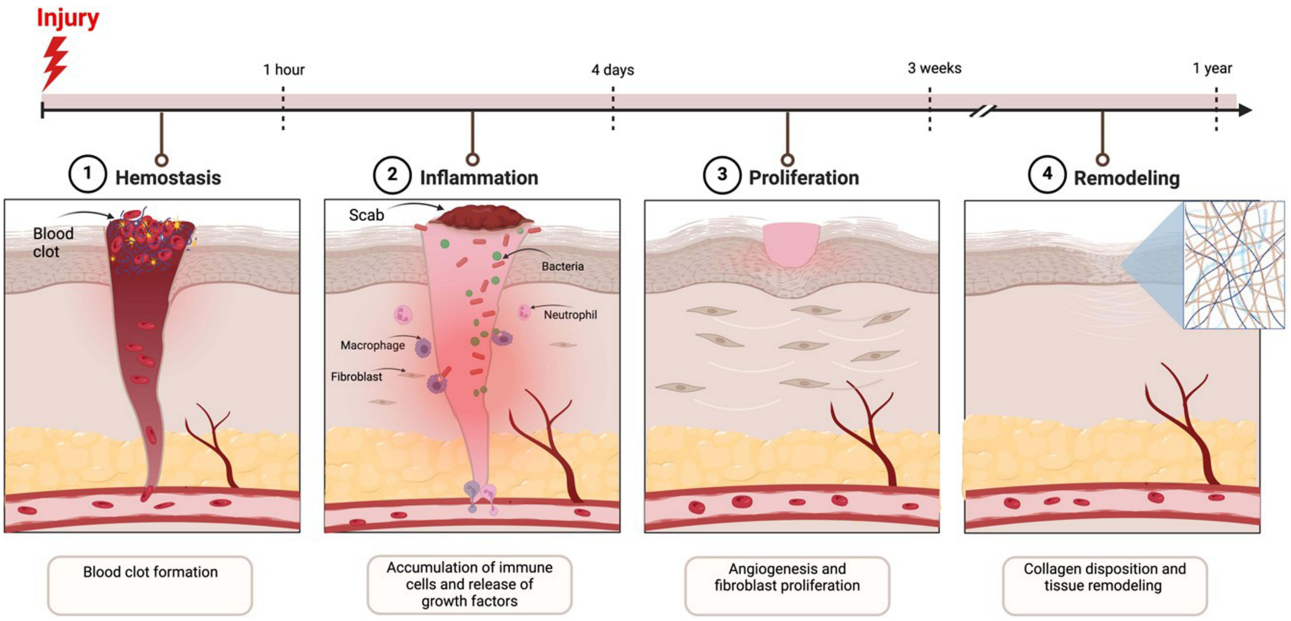

Figure 1 The four stages of the wound healing process and the hallmark of each stage: are (1) hemostasis, (2) inflammation, (3) proliferation and (4) remodeling. Created in Biorender.com.

Wound healing is a complex biological process which involves a series of physiological and biochemical events that are promptly initiated upon skin injury. There are four distinct stages of wound healing: hemostasis, inflammation, proliferation, and remodeling, as illustrated in Figure 1. The initial stage of wound healing ie, hemostasis, starts upon the occurrence of endothelial damage. This stage is characterized by the aggregation of platelets that adhere to the injury site to initiate the clotting cascade and prevent further bleeding during the first 24–48 hours.[4] The fibrin clot formation leads to the second stage of the healing process by attracting inflammatory cells, fibroblasts and growth factors and promoting tissue regeneration lasting for around 4 days.[5] By the end of the inflammations stage and in the proliferation stage, eschar (scab) forms on the surface of the wound. The inflammatory components contribute to increasing blood flow to the injured area, swelling and redness. Furthermore, growth factors released by inflammatory cells stimulate further cell migration and proliferation of fibroblasts and endothelial cells to remove dead tissue which typically lasts from 5 to 20 days post-injury.[6] During the fourth stage, disorganized collagen, produced by fibroblasts, promotes wound contraction and the formation of fresh skin.[5] The duration of the final phase may extend from days to a year or beyond, depending on the complexity of the wound. Given the intricate nature of the wound healing process, delayed wound healing or excessive healing, ie, scar formation, might occur at any stage impacting the structure and function of the wounded area.

Current interventions for wound management vary depending on the severity of the injury. For most skin wounds, hospitalization is not required; however, infection, deformity or hemorrhage might delay healing and cause complications.[7] Conventional wound dressings are typically comprised of cotton, bandages, and gauze which are commonly utilized in clinical settings to prevent bacterial and fungal invasion of the body, primarily due to their cost-effectiveness and absorbency properties. However, conventional dressings potentially delay the wound healing process by isolating the open wound while causing dehydration by absorbing exudate from the wound surface.[6]

Bacteria are an essential part of a healthy skin's ecosystem. However, in the event of an injury, they can travel from the surface to penetrate areas where they do not normally reside, resulting in an imbalance that leads to infection of the skin wound.[8] Microbial infection is one of the key factors that can impair the wound healing process, complicate the recovery, and increase the cost of wound care. Bacterial invasion can impair the typical progression of wound healing and may lead to disfigurement of the wound site which might pose a serious threat to the patient's survival. Thus, the development of novel concepts to enhance tissue regeneration and prevent infections is key to managing wounds effectively. Interventions,

including but not limited to devices, dressings, drugs, and delivery systems, were extensively investigated to facilitate enhanced wound healing using cost-effective and biocompatible approaches. Ideally, a wound dressing must maintain close contact with the wound, control exudates and limit inflammation all while maintaining a moist environment.[9–11]

Electrospinning is a widely used technique that allows the fabrication of micro- or nano-sized fibers for various biological and nonbiological applications.[12] Electrospun nanofibers present great potential for wound dressing applications as they exhibit a structure that can support the wound while providing a microenvironment for cell adhesion and migration throughout all the stages of the healing process.[3,6] Additionally, the nanofibrous architecture emulates the porous nature of the extracellular matrix (ECM) which facilitates epithelial cell adhesion, migration and differentiation.[13] Moreover, due to their high surface area, electrospun fibers can absorb exudates from the wound site; while, at the same time, preventing external microbial infection and facilitating localized delivery of therapeutic agents.[14]

Natural polymers, including for instance, cellulose, collagen chitosan and alginate, are mainly derivatives from animal or plant sources and generally exhibit high biocompatibility and low toxicity but often suffer from poor solubility and instability.[6,15–17] Poly lactide-co-glycolic acid (PLGA), polycaprolactone (PCL), and polyvinyl pyrrolidone (PVP) are examples of synthetic polymers that are widely used for electrospinning due to their mechanical properties, biocompatibility, and stability.[18] PLGA is a hydrophobic FDA-approved copolymer that has been widely investigated due to its favorable properties including biocompatibility, tunable degradation rate, and ease of fabrication.[19] Upon hydrolysis, the ester link present in PLGA breaks releasing lactic acid and glycolic acid monomers. Lactate, as a biodegradable metabolite, plays a crucial role in diverse biochemical processes and can elicit therapeutic benefits by promoting angiogenesis and wound healing. For that reason, it has been reported that PLGA, on its own, might have wound-healing properties via accelerating angiogenesis.[3,20] On the other hand, PVP is an FDA-approved hydrophilic polymer with an amorphous nature, biocompatible and biodegradable.[21] Owing to its high porosity, PVP nanofibers have an ultrarapid release rate of water-soluble drugs as well as a high surface-to-volume ratio.[22]

The use of nanofibrous systems for wound dressing applications has gained significant attention due to the pressing need for novel approaches to accelerate wound closure. Gilchrist et al reported developing biodegradable PLGA nanofibers co-loaded with fusidic acid and its sodium salt to prevent orthopedic implant-associated infections.[23] In a rodent model, the co-loaded nanofibers significantly reduced MRSA colonization on titanium implants by 99.9%; while the treated implants showed a reduced inflammatory response compared to controls.[23] In another study, Wang et al developed a PLGA-based nanofibrous scaffold loaded with zinc oxide nanoparticles (ZnO NPs) and vascular endothelial growth factors (VEGF) for wound dressing applications.[10] The formulation containing both ZnO NPs and VEGF showed an early wound contraction and better tissue organization before injury.[10]

Fusidic acid (FA) is a narrow-spectrum semisynthetic agent derived from the fungus *Fusidium coccineum* that is available in various dosage forms to treat skin infections. Fusidic acid is principally active against *staphylococci*, including methicillin-resistant strains (MRSA), as well as other Gram-positive bacteria and a limited number of Gram-negative bacteria.[24,25] Lidocaine (LDC) is a widely used pre- and postoperative local anesthetic and numbing agent that can be applied directly on the skin to reduce pain. Due to its hydrophilicity, LDC has a short half-life in vivo making the use of a polymeric carrier an attractive strategy to prolong its release.

This study investigates the therapeutic potential of FA in combination with LDC in two separate formulations; PLGA/PVP-based nanofibrous system and PVP-based nanofibers to evaluate their effectiveness in accelerating the wound closure of an infected open wound. Due to the distinctive nature and unique physicochemical properties of the polymers utilized, each resulting formulation is designed for a different onset of action. The PLGA/PVP-based system is intended for a once daily more prolonged drug release over 24 hours period; while, on the other hand, PVP-based nanofibers were formulated for a more rapid release of both drugs upon contacting the site of application. The aim is to provide two formulations with the potential to be used as over-the-counter (OTC) dressings for wounds.

Materials and Methods

Materials

Fusidic acid sodium salt (FA), lidocaine hydrochloride monohydrate (LDC), Ethanol (absolute, ≥ 99.8%) and PVP with a molecular weight of ~1,300,000 were all purchased from Sigma-Aldrich (St. Louis, MO, USA). Purasorb® PDLG 5010

 https://doi.org/10.2147/IJN.S467469

(MW 153 kg/mol), a copolymer of PLGA 50:50 was obtained from Corbion (Purac Biomaterials, Gorinchem, Netherlands). Acetonitrile (ACTN, ≥99.9% for HPLC) was purchased from Scharlau (Barcelona, Spain). Phosphate-buffered saline (PBS) was prepared by dissolving PBS tablets, obtained from Sigma-Aldrich, in the corresponding amount of distilled water generated via the Milli-Q® IQ 7005 Purification System (Millipore SAS, Molsheim, France). pH adjustment to 6.8 was carried out using 0.1N hydrochloric acid (HCL) that was purchased from Scharlau.

Bacterial strains were purchased from the American Type Culture Collection (ATCC) (Manassas, VA, USA) as reference bacteria, including *Staphylococcus aureus* (*S. aureus*; ATCC 29213), *Escherichia coli* (*E. coli*; ATCC 25922), *Pseudomonas aeruginosa* (*P. aeruginosa*; ATCC 27853), and *methicillin-resistant Staphylococcus aureus* (*MRSA*; ATCC 43300). The study also included other bacterial strains that were isolated clinically, such as *E. coli* (1060) and *P. aeruginosa* (7067). The bacterial strains were cultured on Mueller–Hinton agar (MHA) and Mueller-Hinton broth (MHB) obtained from Scharlau (Barcelona, Spain) and prepared according to the manufacturer's instructions. Distilled water was generated using a Milli-Q® IQ 7005 Purification System.

Animal Study

Adult animals (Swiss mice) weighing 25–30 grams were obtained from the animal house of the Faculty of Pharmacy, King Abdulaziz University, Jeddah, Saudi Arabia. The in vivo study protocol was approved by the Local Committee of Ethics of Research on Living Creatures in King Abdulaziz City for Science and Technology- Institutional Review Board (KACST-IRB, no. IRB 23006), in adherence with the Declaration of Helsinki, the Guiding Principle in Care and Use of Animals (DHEW production NIH 80–23) and the Standards of Laboratory Animal Care (NIH distribution 85–23, reconsidered in 1985). Animals were kept in cages housing 4 animals, adapted for at least 2 weeks in naturally controlled enclosures (20 ± 1°C and a 12/12-h dark/light cycle) and fed food pellets and tap water ad libitum.

Methods

Preparation of the Nanofibrous Systems

FA/LDC-Loaded PLGA/PVP Fibers

10% (w/v) PVP and 25% (w/v) PLGA were separately dissolved in ethanol and acetonitrile, respectively, and then stirred at 500 revolutions per minute (rpm) for one hour at ambient temperature using magnetic stirrer. LDC was mixed with PVP, while FA was combined with PLGA. The resulting solutions were then stirred for an additional hour to obtain homogeneous solutions. A mixture of PVP and PLGA (in a 1:3 ratio) was formed to produce the nanofibers containing both LDC and FA at a final concentration of 1% (w/v) per drug. For the fabrication of the monoaxial fibers, the Spraybase® electrospinning instrument (Spraybase®, Dublin, Ireland), which comprised of a syringe pump, high power voltage supply and a collection surface, was used at 37°C and humidity conditions ranging between 30% to 40%. The solution was then transferred into a 5 mL plastic syringe fitted with a 20-gauge needle streaming the mixture at 0.8 mL/hour flow rate, 15 cm tip-to-collector distance and 10–12 kV voltage range. The yielded nanofibers were collected from an aluminum foil that covered the metallic collector. Similarly, drug-free (ie, blank) PLGA/PVP fibers were prepared in the exact electrospinning conditions but without the addition of any drug and the voltage was set at 7–8 kV.

FA/LDC-Loaded PVP Fibers

The polymeric solution was prepared by dissolving 10% (w/v) PVP in ethanol which was then kept stirring for one hour at room temperature. FA was added to the solution while the mixture was maintained under continuous stirring, followed by the addition of LDC to create a homogeneous solution. The drug-loaded and drug-free (ie, blank) PVP nanofibers were fabricated using the Spraybase® electrospinning instrument following the same conditions detailed in the previous section; except the size of the streaming needle (18-gauge).

Morphological Characterization of the Fabricated Nanofibers by Scanning Electron Microscopy (SEM)

The morphology of the nanofibers was imaged using an SEM (JSM-IT500HR SEM, Jeol Inc., Peabody, MA, USA). The nanofibers were collected on aluminum foil and coated with a 2 nm layer of platinum using a JEC-3000FC auto fine coater (JEOL Inc., Peabody, MA, USA) to enhance conductivity and imaging quality. The samples were then imaged

with the SEM, with measurements taken at an accelerating voltage of 5 kV. The average fiber diameters were calculated from measurements taken on 70 individual fibers using ImageJ software (National Institute of Health, MD, USA). Results were analyzed by OriginPro 2021 (OriginLab Corporation, Northampton, MA, USA).

Fourier-Transform Infrared Spectroscopy (FTIR)

The molecular structures of PVP, PLGA, FA, LDC, their physical mixtures PM1 (PLGA/PVP/FA/LDC in a ratio of 3:1:1:1) and PM2 (PVP/FA/LDC in a ratio of 10:1:1), blank fibers, and drug-loaded fibers were determined by FTIR Thermo smart ATR IS20 Spectrometer (Thermo Fisher Scientific, Waltham, MA, USA) at wavenumber range between 4000 and 600 cm^{-1} and 32 scans with a resolution of 4 cm^{-1}.

X-Ray Diffraction (XRD)

The X-ray diffractogram was used to evaluate the crystallinity and amorphous structure of FA, LDC, PVP, PLGA, PM1 (PLGA/PVP/FA/LDC in a ratio of 3:1:1:1) and PM2 (PVP/FA/LDC in a ratio of 10:1:1), blank fibers, and drug-loaded fibers by Rigaku Miniflex 300/600 (Tokyo, Japan) with Cu Kα radiation (λ = 1.5148 227 Å) and a voltage of 40 kV and current of 15 mA. The samples were scanned between 3◦ and 60◦ diffraction angles (2θ) at 5◦/min.

Quantification of FA and LDC Using High-Performance Liquid Chromatography (HPLC)

Both drugs were quantified using the Waters e2695 HPLC system that consists of a Waters® 717 plus autosampler, Waters 600 binary pump, and Waters 2489 UV/detector (Waters Technologies Corporation, Milford, MA, USA). The drugs were separated by an isocratic elution of a mobile phase of triethanolamine (1%, adjusted by formic acid to pH 3.9), and acetonitrile at a ratio of 30% and 70%, respectively, and a Waters XBridge C_{18} column (4.6 mm × 250 mm, 5 µm), with a temperature that was maintained at 20°C. The flow rate of the mobile phase was adjusted at 1 mL/min, the injection volume was kept at 10 µL, and the detection was achieved at a wavelength of 210 nm.

For samples containing PLGA and PVP, which were dissolved in ACTN, serial dilutions of the following concentrations were used: 200, 100, 50, 25, 12.5, 6.25 and 3.125 µg/mL were used to develop calibration curves for both drugs according to the method above. Similarly, for FA and/or LDC in PVP samples, that were dissolved in PBS, serial dilutions were conducted to obtain solutions of 1000, 500, 250, 200, 100, 50, 25, 12.5, 6.25 and 3.125 µg/mL.

Assessment of the Encapsulation Efficiency (EE%) and Drug Loading (DL)

The DL and EE% of FA/LDC-loaded PLGA/PVP fibers were assessed by dissolving the fibers (10 ± 0.53 mg, n=3) in 5 mL ACTN for four hours at ambient temperature until full dissolution was achieved. Similarly, the DL and EE% of the FA/LDC PVP fibers were quantified by dissolving the fibrous system (10.4 ± 1.1 mg, n=3) in 5 mL PBS (pH 6.8), for four hours at room temperature. Samples from both fibrous systems were subjected to the previously established HPLC-based method detailed in 1.2.6. and the EE% and DL were calculated according to Alsulami et al[26] using the following mathematical equations:

$$EE\% = \frac{\text{Actual drug amount}}{\text{Theoretical drug amount}} \times 100 \quad (1)$$

$$DL = \frac{\text{Entrapped drug amount}}{\text{Fibers Weight}} \quad (2)$$

The results were shown as the mean ± standard deviation (SD) of three replicates.

In vitro Assessment of the Release Rate by Franz Diffusion

The release characteristics of the drugs from the fabricated nanofibers were investigated in vitro via the Franz diffusion cell system (PermeGear, Hellertown, PA, USA) as a modified protocol from Alzahrani et al.[27] The study was conducted by placing a semipermeable membrane with a molecular weight cut-off range of 12–14 kD (Spectra/Por®, Spectrum Laboratories Inc., Ranch Dominguez, CA, USA) on the respective Franz diffusion cells. Each receptor chamber was filled with 3 mL of PBS (pH 6.8); while 1 mL of PBS was added to the donor chambers. Predefined amounts of the nanofibrous systems were positioned on the donor part and the Franz cells were maintained covered with parafilm®

throughout the experiment. The study was performed under a temperature-controlled environment of 37°C, using a circulating water bath to simulate the surface temperature of the skin. Additionally, the diffusion medium was agitated at a speed of 500 rpm. 100 µL samples were collected from each receptor chamber, which was subsequently replenished with fresh buffer to preserve the sink conditions, at the following time points: 0.5, 1, 2, 4, 6, 8, 24 and 48 hours for the FA/LDC-loaded PLGA/PVP fibers and 0.5, 1, 2, 4, 6 and 24 hours for the FA/LDC-loaded PVP nanofibers. The collected samples were analyzed using the developed HPLC protocol in 1.2.6., and the percentage of cumulative release for each drug was quantified according to the equation below:

$$\text{Cumulative Release\%} = \frac{\text{Cumulative drug amount}}{\text{Theoretical drug amount}} \times 100 \quad (3)$$

The results were shown as the mean ± SD of at least three replicates.

In vitro Cell Viability Study

Cells Subculturing

A human skin fibroblast cell line (HFF-1) was utilized to assess the cytotoxicity of the applied drugs. HFF-1 was obtained from the American Type Culture Collection (ATCC) under catalogue number SCRC-1041 (Manassas, VA, USA). The cell line was routinely cultured and maintained in high glucose Dulbecco's Modified Eagle Medium (DMEM) for HFF-1 cell line, 10% fetal bovine serum (FBS), and 1% antibiotic solution composed of penicillin (10,000 IU/mL), streptomycin (10 mg/mL), and amphotericin B (25 µg/mL), which were all bought from Sigma-Aldrich (St. Louis, MO, USA). The cell viability assessment of tested compounds was conducted using MTS assay.

Cytotoxicity Assay

The tested materials (FA, LDC and their drug combination) were dissolved in DMEM and six serial dilutions were applied to the HFF-1 cells, starting with 500 µg/mL down to 16 µg/mL. The cytotoxicity of the two drugs was assessed using cell titer 96® aqueous one solution cell proliferation assay (MTS kit), which was purchased from Promega (Southampton, UK), following the modified method of Alsulami et al.[26] Briefly, HFF-1 cells were seeded in 96-well plates with a density of 1.5×10^4 cells per well, followed by their incubation at 37°C overnight. After cells adhered, FA, LDC and their drug combination (with a 1:1 ratio) were added with different concentrations for 24- and 48-hours at 37°C. Negative control (completed DMEM only) and positive control (0.2% triton x-100) were used as experimental controls. After the proposed incubation time, cells were washed with sterile phosphate-buffered saline (PBS, pH 7.4) and then 100 µL of complete DMEM medium were added with 20 µL of MTS reagent per well. After that, cells were incubated for 3 hours in a cell culture incubator. The absorbance at 492 nm was recorded using Cytation 3 absorbance microplate reader (BIOTEK Instruments Inc., Winooski, VT, USA). The percentage of cellular viability was calculated using the following equation:

$$\text{Cell Viability}(\%) = \frac{(S - T)}{(H - T)} \times 100 \quad (4)$$

where S is the absorbance of the cells treated with the tested drugs, T is the absorbance of the negative control, and H is the absorbance of the positive control.

Assessment of the Minimum Inhibitory Concentration (MIC) of FA and LDC

The minimum inhibitory concentration (MIC) values of FA, LDC, and their combination were determined using the broth microdilution method, which adheres to the Clinical and Laboratory Standards Institute guidelines (CLSI).[28] The drugs were prepared by two-fold serial dilutions ranging from 1000 to 7.8 µg/mL and added to 96-well microtiter plates. Then, the bacterial inoculums of *S. aureus* (ATCC 29213, *MRSA* – ATCC 43300), *E. coli* (ATCC 25922 and clinical isolate 1060), and *P. aeruginosa* (ATCC 27853 and clinical isolate 7067) were adjusted to a McFarland standard of 0.5, giving a cell density of 1.5×10^8 CFU/mL, and added to 96-well microtiter plates. Drug-free wells were used as growth controls, while wells containing only MHB medium were used as negative controls. Then, 96-well microtiter plates were incubated overnight at 37°C with continuous shaking at 160 rpm. The lowest concentration with no visible growth or

turbidity was considered the MIC, and bacterial growth inhibition was measured at a UV absorbance of 600 nm using a PowerWave XS2 plate reader (bioMérieux, Marcy L'Etoile, France). Results were expressed as the mean ± SD of three replicates.

Determination of the Antibacterial Activity of the FA/LDC-Loaded PLGA/PVP and FA/LDC-Loaded PVP Fibers

The antibacterial activity of FA/LDC-loaded fibers was assessed using an agar-diffusion assay following a modified approach of Mutlu et al.[29] Bacteria that exhibited antibacterial activity in the MIC test were tested against various fiber systems. MHA plates were inoculated with 100 µL of 1.5×10^8 CFU/mL of *S. aureus*, ATCC 29213, *MRSA* – ATCC 43300, *E. coli*, ATCC 25922, and clinical isolate 1060. Electrospun FA/LDC-loaded PVP fibers, FA/LDC-loaded PLGA/PVP fibers, blank PVP fibers, and blank PLGA/PVP fibers were weighed and cut at certain weighs that represent a drug loading of 80 µg/mg for FA, then placed over plates. To ensure the validity of the test, the FA/LDC inhibition zone was evaluated, and 20 µL of the mixed drugs were added to sterile microbiological discs as an experimental control. All plates were incubated overnight at 37°C. After incubation, the diameters of the inhibited zones were measured in millimeters (mm) by a digital micrometer. All results represent the mean ± SD of three replicates.

In vivo Animal Study

Animal Preparation and Superficial Wound Infection

The in vivo model infection process, detailed by Pérez et al[30] was followed. The colonization was initiated via incisional abrasion using an infective dose of *S. aureus* 3×10^8 CFU/mL. Bacterial growth began within the first four hours, following a self-limiting pattern, with bacterial maturation reaching 10^5 CFU/mL within 48 hours post-inoculation and persisting for a clinical duration of 14 days. A superficial abrasion was created on 44 mice under anesthesia (Ketamine/Xylazine IP at 80 mg/kg + 5 mg/kg). The skin was disinfected with 70% alcohol, and abrasions were made using a scalpel (number 11) until redness appeared and the epidermis was visibly lost. Wounds were approximately 1 cm in diameter and were located in the dorsal area. Wounds were infected with the inoculum previously obtained for 24 hours. To determine the bacterial burden of the wounds throughout the experiment, swabs and digital pictures were taken on days 1, 3, 6, 8, 10 and 14. Samples were studied using routine microbiological procedures,plated on MHA and the number of bacteria was quantified by serial dilution in PBS buffer and expressed as CFU/mL and log10. The threshold value for an established skin infection by *S. aureus* was 10^5 CFU/mL. All experiments were carried out 3 times and a reduction in the number of CFU/mL of 6 log10 was considered indicative of bactericidal activity.[31]

Treatment of the Infection

The animal experiment was designed to fulfill the objective of the investigation. Accordingly, a total of 44 mice were distributed to 11 groups (n=4 per group), untreated group (infected, no treatment), commercial Fucidin cream group (infected, treated), commercial Lidocaine cream group (infected, no treatment), PLGA/PVP fibers groups: Blank (infected, no treatment), FA-loaded PLGA/PVP, FA/LDC-loaded PLGA/PVP (infected, treated) and LDC-loaded PLGA/PVP (infected, no treatment) and PVP fibers groups: Blank (infected, no treatment), FA-loaded PVP, FA/LDC-loaded PVP (infected, treated) and LDC-loaded PVP (infected, no treatment).

Macroscopic Observations

Mice were monitored on days 1, 3, 6, 8, 10 and 14 to study wound healing in response to the infection and the different therapies. Digital images were taken using the Canon PowerShot A630© camera to assess the wounds. The progression of the wound, estimating the days to get a reduction of 50% of the size and the loss (detachment) of the crust (LC, time in days required to fall off) were evaluated.[31]

Microbiological Evaluation

Swabs of the wounds were carried out. The swab end was then sliced and inserted in a tube with 2 mL of sterile saline followed by mixing the tube on Vortex to release the *S. aureus*. Serial 100-fold dilutions of the cell suspension were cultured on MHA plates at 37°C for 20 hours. Finally, *S. aureus* colonies were counted.

PLGA/PVP and PVP Fibers Treatment

PLGA/PVP and PVP fibers containing FA, LDC alone or combined were applied to the mice wounds while commercialized Fucidin cream (Fusibact™; Jamjoom Pharma, Jeddah, Saudi Arabia) and Lidocaine cream (Rialocaine®; Riyadh Pharma, Jeddah, Saudi Arabia) were applied to the mice wounds during the experiment. Both formulations were given once daily from day 1 after inoculation to day 14 post-infection.

Statistical Analysis

The EE%, DL, drug release studies, in vitro and in vivo experiments were all conducted with at least three independent replicates with the data presented as the mean ± SD. Statistical analysis was performed using OriginPro® 2021 (OriginLab Corporation, Northampton, MA, USA) and Microsoft Excel 2024 software. The number of CFUs and the score of wound infection were measured three times independently.

Results and Discussions

Morphological Characterization of the Fabricated Nanofibers by Scanning Electron Microscopy (SEM)

The prepared monoaxial drug-loaded and blank nanofibrous formulations were assessed for their surface morphologies. As shown in Figure 2, the nanofibers were fabricated uniformly, presenting smooth, non-porous surfaces without any bead-like defects or irregularities. The observed morphological attributes are considered to meet the preparatory criteria for effective fiber fabrication.[32]

The fiber diameters were measured for blank PLGA/PVP and FA/LDC-PLGA/PVP nanofibers indicating an average diameter of 1117 ± 284 nm and 556 ± 71 nm, respectively. Similarly, the blank PVP had an average diameter of 812 ± 120 nm, while the FA/LDC-PVP fibers measured 291 ± 87 nm. The two nanofibrous systems exhibited a common observation: the blank fibers had larger diameters than the drug-loaded fibers, which aligns with previously reported findings.[23,27,33] The incorporation of both drugs into the polymeric solutions used to fabricate DL fibers altered their conductivity and viscosity, requiring an increase in the applied voltage. The addition of conductive drugs such as FA and LDC to the spinning polymeric solution plays an essential role in altering the optimal electrospinning parameters as increased conductivity results in reduced fiber diameter.[32] Furthermore, using a lower voltage to fabricate the blank fibers (≥ 8 kV), compared to the dual drug-loaded fibers (≥ 10 kV), facilitated the stabilization of the spinning jet yielding nanofibers with larger diameter.[32]

Fourier-Transform Infrared Spectroscopy (FTIR)

FTIR spectroscopy was used to monitor the formulation's stability and ensure that the polymer structure remained intact after drug incorporation, as any significant changes in the polymer's characteristic peaks could indicate degradation or structural modification caused by the drug loading process. Both formulations in Figures 3A and 3B showed an O-H broad peak at 3650–3500 cm^{-1} and a C=O absorption at around 1750–1650 cm^{-1} in the samples (PVP, PM1, PM2, blank fibers, and drug-loaded fibers), which could confirm the presence of PLGA and PVP polymers in both formulations. PM1 and PM2 reflect a physical combination of all the drug-loaded nanofibers components with no significant shifts or new peaks. The results were consistent with those of the pure components presented in Table 1. The low intensities of FA and LDC peaks could be attributed to the ratio of PM1 (3:1:1:1) and PM2 (10:1:1).

The FA/LDC-PLGA/PVP (Figure 3A) showed stretching vibration peaks of carbonyl in the PLGA structure at 1750 cm^{-1}, in addition to a small peak at 1660 cm^{-1}, which revealed C=O in PVP. Otherwise, the drug-loaded and blank PVP fibers, which contain PVP only, showed a response of carbonyl peak that appeared in the region of 1650 cm^{-1}. In addition, the C-O-C spectrum disappeared in Figure 3B at 1166 cm^{-1} and 1085 cm^{-1}, which belongs to the stretching vibration of ester linkages in PLGA polymer. The results are consistent with the previous report by Fan et al.[38] Comparing drug-loaded and blank fibers in both formulations, it was observed that the spectral intensity at 1750 cm^{-1} and 1660 cm^{-1} increased due to the incorporation of the drugs, as they also contain carbonyl functional groups. Furthermore, the presence of small peaks in the fingerprint area (900 to 600 cm^{-1}) suggests that the drugs are loaded

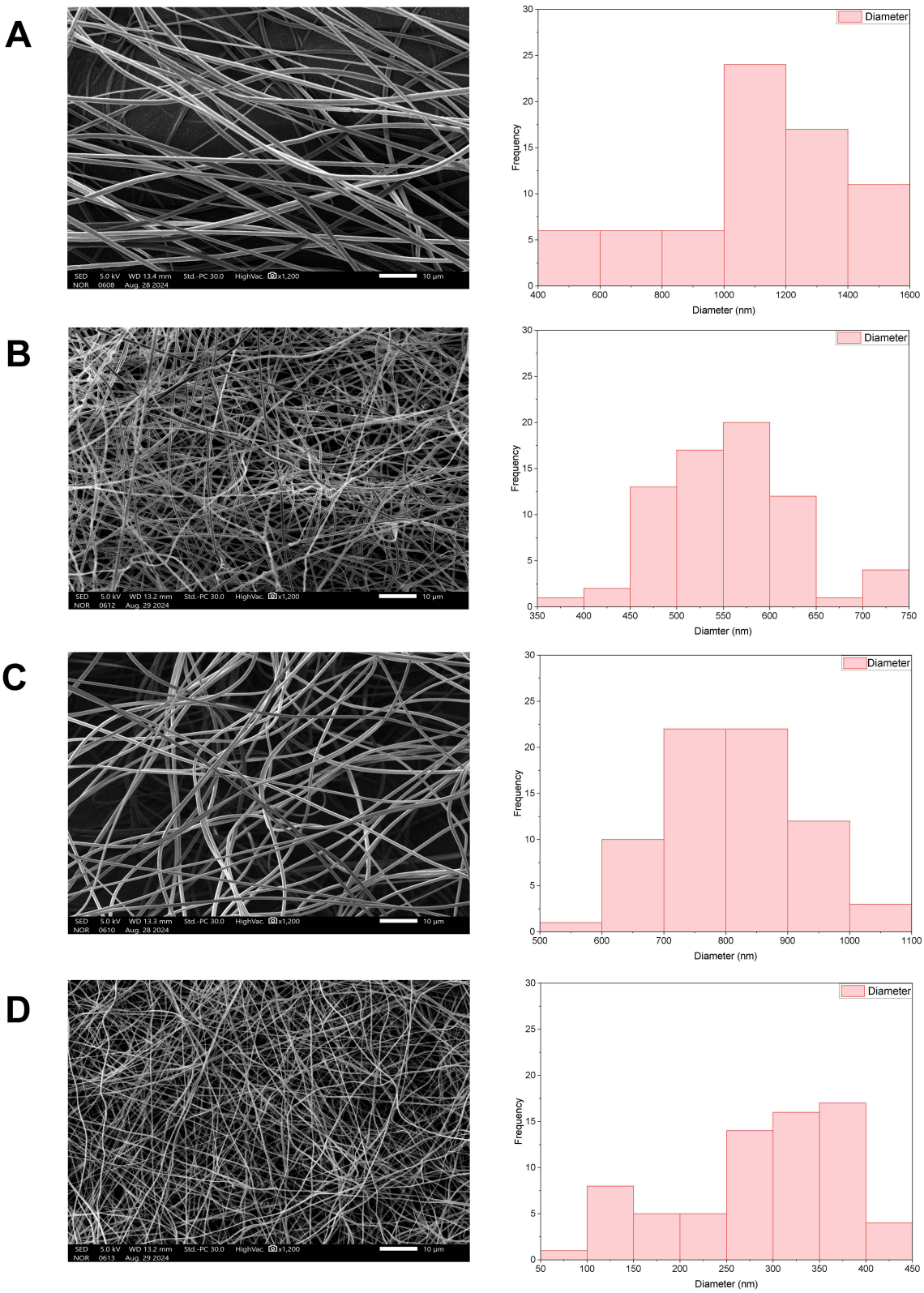

Figure 2 Surface morphologies of blank and drug-loaded monoaxial nanofibers under the scanning electron microscopy (SEM) (**A**) blank PLGA/PVP, (**B**) FA/LDC-PLGA/PVP, (**C**) blank PVP and (**D**) FA/LDC-PVP, as well as their corresponding diameter distribution charts. The size distribution of the blank and drug-loaded nanofibers was measured from 70 different fibers. PLGA; poly lactide-co-glycolic acid, PVP; polyvinylpyrrolidone, FA; Fusidic acid sodium salt, LDC; Lidocaine hydrochloride monohydrate.

https://doi.org/10.2147/IJN.S467469

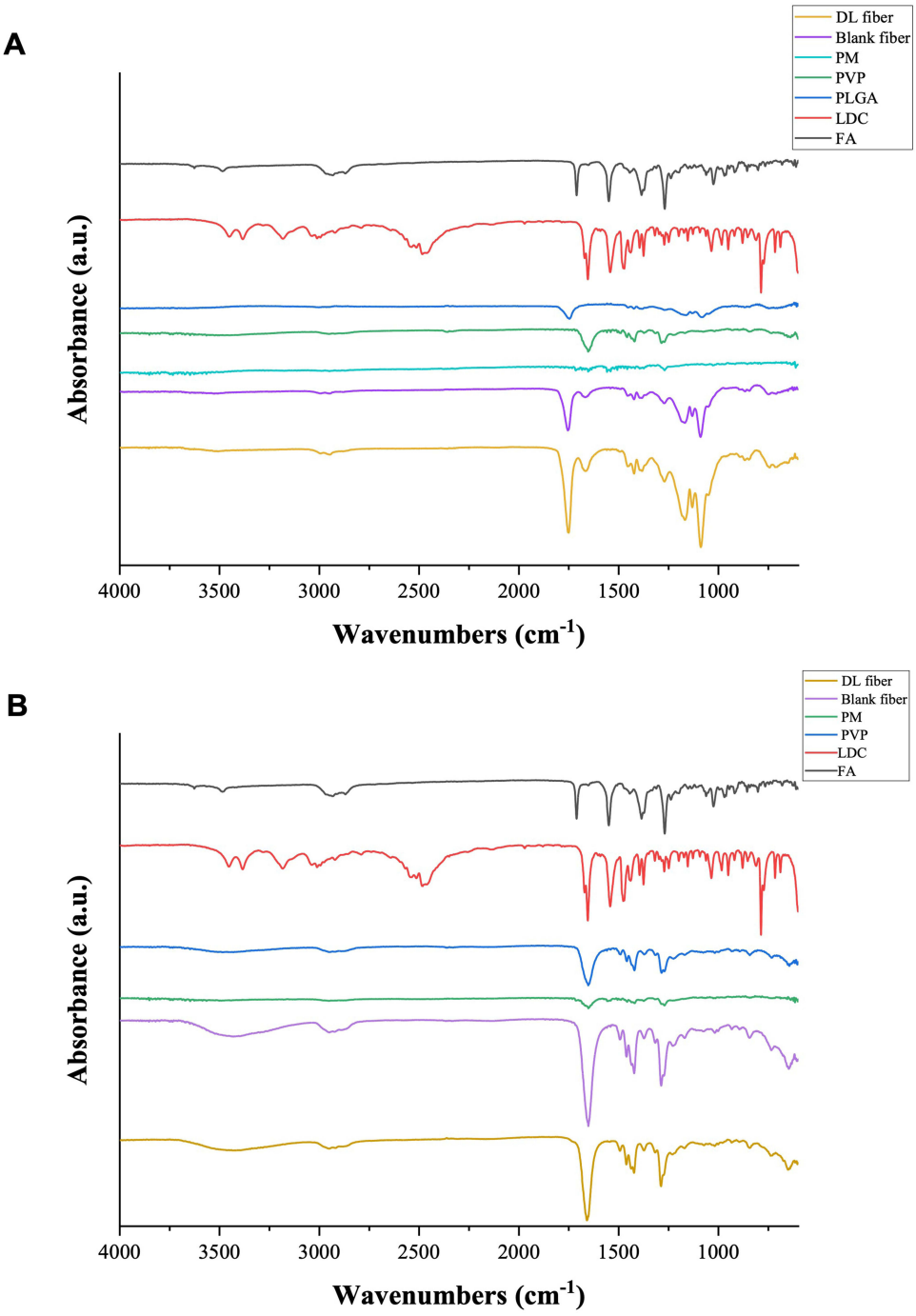

Figure 3 Fourier-Transform Infrared Spectroscopy (FTIR) spectrums for (**A**) PLGA, PVP, Physical mixture 1 (PM1), Lidocaine, Fusidic Acid, Blank and FA/LDC-PLGA/PVP (drug-loaded (DL)) fibers, and (**B**) PVP, physical mixture 2 (PM2), Lidocaine, Fusidic Acid, Blank and FA/LDC-PVP (DL) fibers. PM1, composed of PLGA, PVP, FA, and LDC, and PM2, composed of PVP, FA, and LDC, were prepared in specific ratios of (3:1:1:1) and (10:1:1), respectively. PLGA; poly lactide-co-glycolic acid, PVP; polyvinylpyrrolidone, FA; Fusidic acid sodium salt, LDC; Lidocaine hydrochloride monohydrate.

inside the nanofibers, which belong to the C-H groups of substituted benzene. The findings align with a previously published study by Alzahrani et al.[27]

In summary, with no notable chemical interactions found, the FTIR analysis indicated the effective integration of all components into the drug-loaded nanofibers, suggesting that the drugs were physically blended within the fiber matrix and electrospun without changing their chemical structures.

Table 1 Fourier-Transform Infrared Spectroscopy (FTIR) Characteristic Peaks of Pure PLGA, PVP, FA and LDC

Sample	Wavenumber (cm^{-1})	Functional Group	Ref.
PVP	3450	O-H stretching	[34]
	2950	C-H asymmetric stretching vibration peaks	
	1652	C=O stretching vibration from pyrrolidone	
	1489, 1457, 1432	C-H bending vibration of aliphatic	
	1285	C-N stretching from pyrrolidone	
PLGA	3652	O-H stretching of hydroxyl groups	[35, 36]
	2998	C-H stretching vibration peaks	
	1746	C=O stretching of carbonyl present in both lactic acid and glycolic acid units	
	1452, 1423, 1381	C-H bending of methyl and methylene Groups in the lactic acid and glycolic acid units	
	1161	C-O stretching of ester linkages	
	1079	C-O-C stretching of ester linkages	
FA	3484	O-H stretching	[37]
	2932 and 2869	C-H symmetric and asymmetric stretching	
	1710	C=O stretching	
	1549	C=C stretching	
	1385	C-H bending vibration of methyl	
	1269	C-O stretching vibration	
	1024–865	C-H vibration of the aromatic ring	
LDC	3383	N-H stretching of secondary amine	[38]
	3181	Aromatic C-H stretching	
	3035–2920	Aliphatic C-H Stretching	
	1655	C=O Stretching of carbonyl in the amide group	
	1542	C=C stretching vibrations in the aromatic ring	
	1471	N-H bending of amide band	
	1271	C-N Stretching of amine and amide groups	

Abbreviations: PLGA, poly lactide-co-glycolic acid; PVP, polyvinylpyrrolidone; FA, Fusidic acid sodium salt; LDC, Lidocaine hydrochloride monohydrate.

X-Ray Diffraction (XRD)

XRD analysis plays an important role in determining the crystalline or amorphous nature of drug-free and drug-loaded nanofiber samples. Such data helps in understanding the stability of the drug in the nanofibers. Figure 4 shows the XRD results of the PLGA/PVP and PVP nanofibrous systems. The amorphous structure was expressed in PVP, PLGA, PM1, PM2, and blank fibers. PM1 demonstrated a broad diffraction peak at 20.1°, which exhibited a relatively higher intensity compared to PM2. The difference could be attributed to the higher ratio of PLGA to PVP in the first mixture, whereas PLGA is absent in the second mixture.

Sharp distinctive peaks were observed at 2θ of 10.9°, 12.8°, 14.3°, 16.5°, 25°, 25.9°, 31.8°, and 33.9° for LDC and 8.2°, 14.2°, 14.9°, 15.5°, 19.5.8°, and 24.7° for FA, indicating for the presence of both drugs in the crystallinity form. The

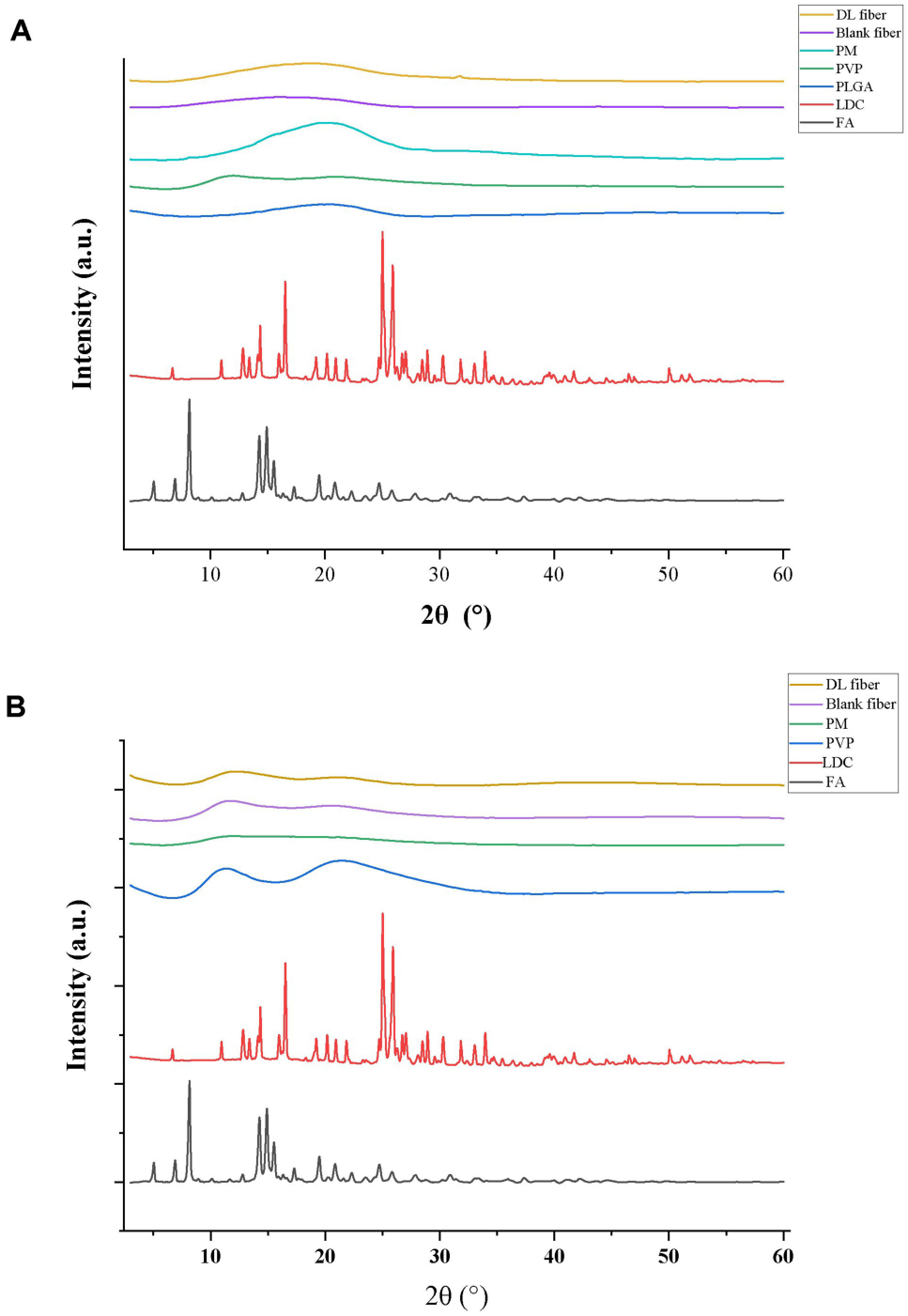

Figure 4 X-ray diffraction (XRD) pattern for (**A**) PLGA, PVP, Physical mixture 1 (PM1), Lidocaine, Fusidic Acid, Blank and FA/LDC-PLGA/PVP (drug-loaded (DL)) fibers, and (**B**) PVP, physical mixture 2 (PM2), Lidocaine, Fusidic Acid, Blank and FA/LDC-PVP (DL) fibers. PM1 was comprised of PLGA, PVP, FA, and LDC; while PM2 was composed of PVP, FA, and LDC. Both PM1 and PM2 were prepared in specific ratios of (3:1:1:1) and (10:1:1), respectively. PLGA; poly lactide-co-glycolic acid, PVP; polyvinylpyrrolidone, FA; Fusidic acid sodium salt, LDC; Lidocaine hydrochloride monohydrate.

observation was also consistent with the previous reports.[27,39–41] Overall, the XRD findings proposed that the electrospinning method has attributed to molecular dispersion of the loaded drugs, which was also reported in multiple previous studies.[42–44]

Quantification of FA and LDC Using High-Performance Liquid Chromatography (HPLC) to Assess the Encapsulation Efficiency (EE%) and Drug Loading (DL)

The development of HPLC methods was crucial for quantifying the DL, EE% and release profiles of FA and LDC from their electrospun nanofibrous systems. Two HPLC methods were developed to separate both drugs; in ACTN to quantify DL and EE measurements for the FA/LDC-loaded PLGA/PVP system, and PBS (pH 6.8) for DL and EE measurements of the FA/LDC-loaded PVP system and the release measurements for both fibrous systems. The ACTN was used to dissolve the PLGA, as it is a hydrophobic polymer. HPLC analysis demonstrated effective separation of FA and LDC, with both drugs being eluted (ie retention time Rt) at 2.9 min for FA and 6.8 min for LDC, as shown in Supplementary Figure 1. Predetermined calibration curves, presented in Supplementary Figure 2, were used to calculate EE% and amount of DL.

The percentages of EE in FA/LDC-PLGA/PVP and FA/LDC-PVP fibers demonstrate the successful incorporation of both drugs in each fibrous system. The loaded PLGA/PVP nanofibers dissolved in ACTN (10±0.53 mg, n=3) had EE% of 92 ± 19% and a DL of 40 ± 8 µg/mg for FA, as well as an EE% of 75 ± 16% and a DL of 32 ± 7 µg/mg for LDC. On the other hand, FA/LDC-PVP exhibited EE% and DL of 101 ± 4% and 85 ± 3 µg/mg, respectively, for FA. For LDC, the encapsulation efficiency was 84 ± 4% with a drug loading of 70 ± 3 µg/mg.

The actual EE% of FA in FA/LDC-PVP slightly exceeded the theoretical amount, which could be due to variations in the deposition of the drugs within the fiber mat; nevertheless, the actual EE% in both formulations closely matched the expected theoretical value (ie, 100%). Despite that, the amount of FA and LDC loaded into PLGA/PVP nanofibers was half the amount in PVP-alone fibers with only 40 ± 8 µg/mg FA and 32 ± 7 µg/mg LDC which could be attributed to the higher polymer-to-drug ratio that was used in the PLGA/PVP fibers (25:10:1:1) compared to the PVP fibers (10:1:1).

In vitro Assessment of the Release Rate by Franz Diffusion

The release dynamics of the drug molecules from their polymeric carriers play an essential role in the process of wound treatment and healing. Franz diffusion cell system was utilized to assess, in vitro, the release profiles of the monoaxial drug-loaded nanofibrous systems. The receptor chambers, where the fibers were placed, contained PBS with a pH of 6.8 to simulate the skin pH in the presence of open wounds which ranges from 6.5 to 8.5.[45] FA/LDC-PLGA/PVP fibers were investigated for 48 hours given the hydrophobic nature of PLGA. As shown in Figure 5A, the released amount of FA in

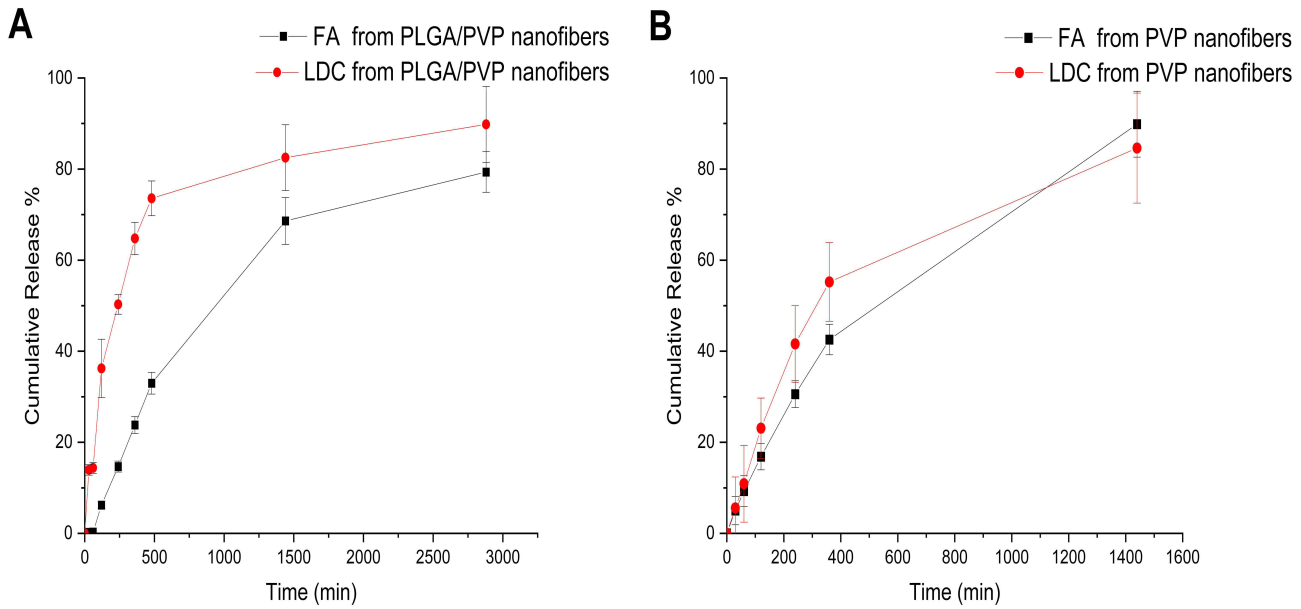

Figure 5 Cumulative Release profile of (A) FA/LDC-loaded PLGA/PVP nanofibers and; (B) FA/LDC-loaded PVP fibers. Results represent the average ± SD (n = 3). PLGA; poly lactide-co-glycolic acid, PVP; polyvinylpyrrolidone, FA; Fusidic acid sodium salt, LDC; Lidocaine hydrochloride monohydrate.

https://doi.org/10.2147/IJN.S467469

the first 30 minutes was merely 1.6% which was followed by a sustained increase, with approximately 50% of the total FA released after 8 hours, 90% after 24 hours, and complete 100% release after 48 hours of incubation. Conversely, LDC showed a faster release pattern with 18% of the drug freed within the first 30 minutes, around 50% within 2 hours and reaching a 100% release rate after 8 hours. The findings indicate the absence of burst drug release, a phenomenon manifested by an initial surge in drug release owing to the rapid drug diffusion from the surface of the nanofibers and often associated with using PLGA in nanoformulations.[46,47] The variation in the release rate between FA and LDC serves the purpose of the formulation; LDC was meant for relieving pain that often accompanies wound sites, and FA was intended for tackling wound infections all while allowing the polymers to exert their wound healing properties.

On the contrary, FA/LDC-loaded PVP nanofibers had different release patterns with 47% of FA released in 30 minutes, 58% within 2 hours, 80% after 6 hours and complete release within 24 hours, whereas only 5% of LDC was released with 30 minutes, 56% after 6 hours reaching 85% release rate after 24 hours (Figure 5B). The release kinetics support the purpose of a more frequent application of the wound dressing, whenever is required, allowing both drugs to exert their effect with faster onset.

Alzahrani et al reported their coaxial nanofibrous system of 8% PVP: FA (shell) and 8% PVP: pirfenidone (core) with slightly different release kinetics of FA. In there, the Franz diffusion cell system was also utilized and only 23% of FA was freed within the first 4 hours and 65% after 24 hours.[27] Upon comparison with the current PVP fibrous system, one can notice that the variation in the fabrication method (monoaxial 10% PVP versus coaxial 8% PVP) might played a fundamental role in the changes in the release behavior between the two formulations; in addition to the intermolecular interaction that could exist between the polymer and the drugs, which would require a further investigation in upcoming studies.

In vitro Cell Viability Study

The cellular and metabolic activity of human dermal fibroblasts (HFF-1 cells) was assessed using the MTS assay following 24- and 48-hour incubation with FA, LDC and their combination. The cell viability assay was performed on HFF-1 human cells as a representative cell line to assess the safety of the drugs. HFF-1 cell line is highly sensitive and can easily be affected by any source of cytotoxicity that might be induced by the applied materials. Two-time points (24- and 48-hours cell exposure) were used to determine the inhibitory concentrations (IC) of both drugs to be taken into consideration later in the in vivo study.

As shown in Figure 6A, the incubation of FA for 24 hours demonstrated that the concentration of the drug ≥ 250 µg/mL on HFF-1 cells represented low cell viability (below 50%), while the lowest applied concentration of 16 µg/mL

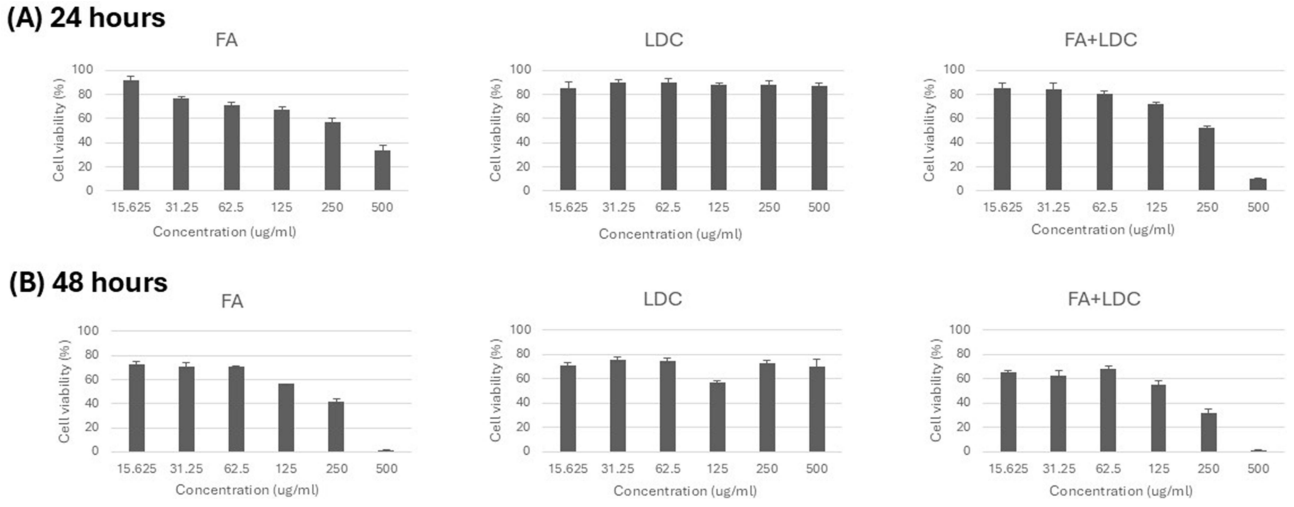

Figure 6 Percentage of Cell variability of HFF-1 with different concentrations of FA, LDC & their combination (1:1 ratio) at two different points: (A) 24 hours and (B) 48 hours. MTS assay results are expressed as cellular viability (%) and presented as the mean ± SD (n = 3). FA; Fusidic acid sodium salt, LDC; Lidocaine hydrochloride monohydrate.

showed highest cell viability of approximately 90% relative to positive control. However, the exposure of FA for 48 hours exhibited low cell viability of HFF-1 cells (< 50%) at ≤ 125 µg/mL, as presented in Figure 6B.

On the other hand, the incubation of LDC with HFF-1 cells for 24 hours showed no reduction in the cell viability below 80% (ie, ≥ 80%) at all applied concentrations (Figure 6A), while extended incubation time of LDC with the human skin fibroblast cells for 48 hours demonstrated lower cell viability (< 80% but > 50%) for the equivalent concentrations as shown in Figure 6B.

The cytotoxicity of the drug combination of FA and LDC with a ratio of 1:1 was also assessed following the incubation with HFF-1 cells for 24 and 48 hours, and results presented in Figure 6A and 6B, respectively. The application of drug combination for 24 hours showed high cell viability (≥ 50%) for all concentrations of ≥ 250 µg/mL, while increased doses of drug combination could induce lower cell viability (< 50%). However, the incubation of drug combination for 48 hours with HFF-1 cells exhibited low cell viability of 50% at ≥ 125 µg/mL.

Overall, the cytotoxicity results for 24 hours demonstrated that the application of the drugs alone or in combinations has no harmful effect on the cell viability when applied at < 125 µg/mL, whereas increasing the dose above 125 µg/mL could induce HFF-1 cells toxicity. Interestingly, the incubation of drug combination exhibited that LDC may hide, normalize, or mask the cytotoxic effect of FA as the reduction in cell viability appeared only at the highest concentration (125 µg/mL) in comparison to 32 µg/mL in free drug. It should be noted that the prolonged incubation time of all applied drugs and their combination to 48 hours demonstrated lower cell viability of HFF-1 cells compared to 24 hours of exposure.

In line with the findings above, a concentration of ≤ 125 µg/mL was selected for further biological studies with the dual drug-loaded nanofiber systems.

Assessment of the Minimum Inhibitory Concentration (MIC) of FA and LDC

The nanofibrous systems possess appealing controlled-release features, higher drug loading at specific sites, and a positive impact on exudate uptake, gas exchange, and moist conditions, which are crucial in facilitating wound healing.[17,48]

The antibacterial inhibitory effects of FA, LDC, and their combination were initially determined using a MIC assay. The results, presented in Table 2, show that FA as a single antibiotic had MIC values of 7.8 µg/mL against *S. aureus* (ATCC 29213), *MRSA* (ATCC 43300), and 125 µg/mL against *E. coli* (ATCC 25922). However, the clinical isolate of *E. coli* 1060 showed a higher inhibitory concentration of 1000 µg/mL. Similarly, *P. aeruginosa* (ATCC 27853 and its clinical isolate 7067) exhibited higher minimum inhibitory concentrations of 1000 µg/mL. In a recently published study, the MIC of FA against *S. aureus* (ATCC 29213) was reported to be < 1 µg/mL and that against *P. aeruginosa* (ATCC

Table 2 The MICs of FA and LDC Alone or in Combination Against S. Aureus (ATCC 29213) MRSA (ATCC 43300), E. Coli (ATCC 25922, Clinical Isolate 1060), and P. Aeruginosa (ATCC 27853, Clinical Isolate 7067). Strains Were Treated with FA, LDC, and Their Combination 1:1 at Concentrations (1000— 7.8 µg/mL). The Results are Shown as Average ± SD (n=3)

Microorganisms	MIC µg/mL		
	FA	LDC	FA/LDC
***S. aureus* – ATCC 29213**	7.8 ± 0	> 1000 ± 0.02	7.8 ± 0
***MRSA* – ATCC 43300**	7.8 ± 0	> 1000 ± 0.03	7.8 ± 0
***E. coli* – ATCC 25922**	≥ 125 ± 0	> 1000 ± 0.03	≥ 125 ± 0
***E. coli* – Clinical isolate 1060**	1000 ± 0.04	> 1000 ± 0.03	≥ 500 ± 0.02
***P. aeruginosa* – ATCC 27853**	1000 ± 0.02	> 1000 ± 0.02	≥ 500 ± 0.01
***P. aeruginosa* – Clinical isolate 7067**	1000 ± 0.07	> 1000 ± 0.01	≥ 1000 ± 0.02

Abbreviations: MIC, minimum inhibition concentration; FA, Fusidic Acid; LDC, lidocaine.

https://doi.org/10.2147/IJN.S467469

27853) was > 512 μg/mL.[27] Moreover, previous studies examined FA using the microdilution method on Gram-positive and Gram-negative bacteria, including Staphylococcus, Clostridium, Corynebacterium, and Neisseria species, revealed that FA has a potent antibacterial activity with MICs ranges of 0.03–1 μg/mL.[24,49]

FA inhibits protein synthesis through binding to elongation FA elongation factor G (EF-G).[25] Furthermore, FA blocks translocation and protein synthesis; thereby, inhibiting bacterial growth through the same mechanism, and is the only antibiotic that functions on this particular target as it does not exhibit cross-resistance to other common antibiotics.[50] In contrast, LDC alone showed no inhibition to any bacterial strains at any tested concentrations (> 1000 μg/mL). Reported data have investigated the potential inhibition of LDC at 1% w/v (ie, 10,000 μg/mL), which is 10-fold higher than the tested concentration at 1000 μg/mL.[51,52] Additionally, no direct synergistic effects of combining LDC with FA were observed against the tested bacteria, except for *E. coli* clinical isolate 1060, which showed a reduction in MIC to 500 μg/mL requiring further investigation.

Determination of the Antibacterial Activity of the FA/LDC-Loaded PLGA/PVP and FA/LDC-Loaded PVP Fibers

The antimicrobial effects of the drug-loaded fiber systems were evaluated using a zone of inhibition (ZOI) assay. Herein, 2 mg of the FA/LDC-PLGA/PVP fibers (to yield DL = 80 μg/mg for FA and 64 μg/mg for LDC), and 1 mg of the FA/LDC-PVP fibers (to yield DL = 80 μg/mg for FA and 70 μg/mg for LDC), were tested against *S. aureus* (ATCC 29213), and *MRSA* (ATCC 43300). The blank PLGA/PVP and PVP fibers were used as negative controls and FA/LDC discs were used as the positive control. The results of the agar diffusion assay are shown in Supplementary Figure 3.

As detailed in Table 3, the FA/LDC-loaded PLGA/PVP fibers showed that the calculated ZOI diameters of 28 mm against *S. aureus* (ATCC 29213) and 32 mm against *MRSA* (ATCC 43300), while the ZOI for the positive control was 33 mm for both bacterial strains. The FA/LDC-PVP fibers showed ZOI diameters of 31 mm and 32 mm against *S. aureus* (ATCC 29213) and *MRSA* (ATCC 43300), respectively. Moreover, its positive control, at comparable concentrations, exhibited a 33 mm ZOI against the same bacterial strains.

The electrospun nanofiber formulations exhibited inhibition zones comparable to their positive control, suggesting that FA has retained its antibacterial efficacy after being electrospun, which is consistent with a reported FA-loaded PLGA fiber systems on sensitive *S. aureus*.[53] Interestingly, the blank PLGA/PVP fibers, here, presented mild inhibition on *S. aureus* strains, which could be attributed to the organic acid compounds in PLGA that might possess antimicrobial activity. It has been reported that external lactic and glycolic acids influence the inhibition of *S. aureus* under low pH conditions.[54,55]

A study by Hamid et al demonstrated that the antibacterial activity of Moxifloxacin-loaded nanofiber systems against different stains, including *S. aureus* (32.33 ± 1.15 mm), *E. coli* (35.67 ± 1.53 mm), and *P. aeruginosa* (36.83 ± 2.56 mm). Additionally, the blank nanofibers exhibited ZOI values between 16 and 19 mm for the same tested strains.[56] Such findings are consistent with the results obtained in the current study, indicating the potential of the developed FA/LDC-PLGA/PVP and FA/LDC-PVP nanofiber formulations in enhancing the wound-healing process of infected wounds.

Table 3 The Antibacterial Activity of FSA/LDC-Loaded PVP Fibers, FSA/LDC-Loaded PLGA Fibers, Blank PVP Fibers, and Blank PLGA Fibers at a Dose Equivalent to 80 μg/Mg Against S. Aureus (ATCC 29213), and MRSA (ATCC 43300). Data Shown are the Diameters of the Zones of Inhibition Measured in Millimeters (Mm). The Results are Shown as Average ± SD (n=3)

Microorganisms	PVP			PLGA/PVP		
	FA/LDC Disc	Drug-Loaded Fibers	Blank Fibers	FA/LDC Disc	Drug-Loaded Fibers	Blank Fibers
***S. aureus* – ATCC 29213**	33 ± 0	31 ± 1	0	33 ± 1	28 ± 1	5 ± 0
***MRSA* – ATCC 43300**	33 ± 1	32 ± 1	0	33 ± 0	32 ± 1	6 ± 0

Abbreviations: FA, Fusidic Acid; LDC, lidocaine.

Evaluation of the Antibacterial Activity of FA/LDC-PLGA/PVP and FA/LDC-PVP Nanofibers Against Infected Wound Animal Model

An animal model was used to evaluate the efficacy of the nanofibers loaded with FA, LDC or their combination against wound infection. Negative control mice received no treatment; while the two groups that were treated with commercialized FA or LDC creams were considered the positive controls. Additionally, blank fibers and single drug-loaded nanofibers were tested as experimental controls. Accordingly, positive controls, blank fibers (PLGA/PVP and PVP), FA-PLGA/PVP, LDC-PLGA/PVP, FA/LDC-PLGA/PVP, FA-PVP, LDC-PVP and FA/LDC-PVP were all administered to each group once daily for 14 days.

Owing to the sensitivity of *S. aureus* to FA, it was used to infect the animals in the study. The level of *S. aureus* infection was kinetically monitored in the wounds of the mice for the duration of the study. *S. aureus* was collected from wounds of each experimental mouse during the day post-inoculation, on days 1, 3, 6, 8, 10 and 14, as shown in Supplementary Figure 4. Moreover, the appearance of the wounds in the animals was documented photographically, and a macroscopic observational assessment was conducted. The assessment, as detailed in Figure 7, covers observations made on days 1, 3, 6, 8, 10, and 14 post-inoculations.

By day 3 post-inoculation, the FA group had a significantly lower count of bacteria compared to other groups. Also, the PVP combination and FA groups had the same pattern (Supplementary Figure 4). By day 6, the FA-PLGA/PVP group demonstrated a significant reduction in bacterial count compared to all other groups. Similarly, the FA/LDC-PVP and FA-PVP groups showed comparable significant reductions (Supplementary Figure 4). By day 14, the FA/LDC-PVP and FA groups exhibited lower bacterial counts than the other groups. Lastly, while commercial FA cream had the highest immediate effect, the FA/LDC-PVP and FA-PVP fibers maintained a sustainable effect over two weeks.

According to the macroscopic evaluation, results, shown in Figure 7, the variations between the two nanofibrous systems were noticeable; current observations indicated that PLGA/PVP-based exhibited a low absorption rate, resulting in residual stickiness that persisted until the following day's dosing. Additionally, due to the hydrophobicity of the PLGA/PVP system, upon applying the next day's dose, the presence of the fibers required physical removal of the fiber remaining's, which might hinder the activity of the naturally-stimulated components of the wound healing process, such

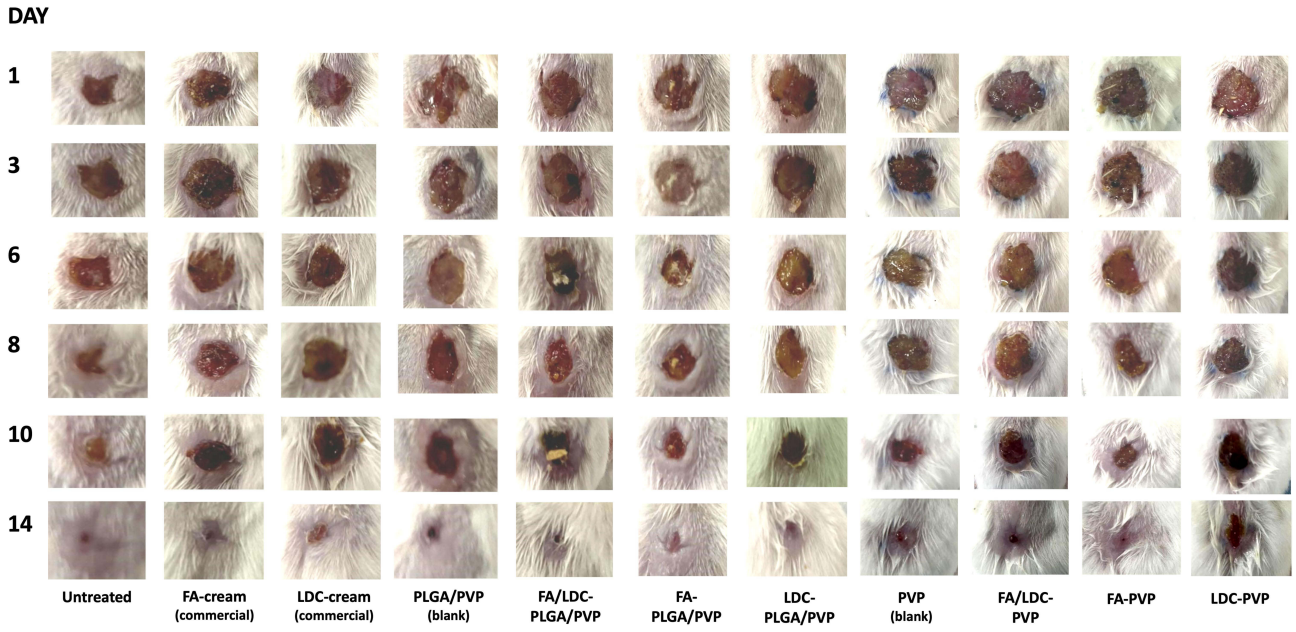

Figure 7 Representative images of the macroscopic evaluation of the wound healing process in an infected wound mice model. Induced wounds were tracked for wound closure in 11 groups over 14 days. PLGA; poly lactide-co-glycolic acid, PVP; polyvinylpyrrolidone, FA; Fusidic acid sodium salt, LDC; Lidocaine hydrochloride monohydrate.

https://doi.org/10.2147/IJN.S467469

as ECM formation. In contrast, PVP-based nanofibers disintegrated upon coming in contact with the open wound which helped in releasing the drugs without negatively affecting the wound healing process.

The in vivo study suggests that the FA/LDC-PVP and FA-cream groups provided the most effective treatment, as evidenced by a relatively earlier wound closure and the significantly lower bacterial counts observed in these groups throughout the experiment. However, PVP fibers demonstrated a preferable feature by having a high absorption within a few seconds, leading to superior drug dissolution compared to the commercially available cream, with the latter attracting dirt and debris in the mice's cages to the open wound and possibly exacerbating bacterial infections.

The pilot study was conducted aiming to investigate the potential impact of the prepared FA/LDC-PLGA/PVP and FA/LDC-PVP nanofibrous systems as wound dressings in an infected wound mouse model. Both formulations were compared against blank fibers, single drug-loaded fibers, and commercially available topical creams to assess their ability to combat *S. aureus* and accelerate the process of wound healing. Both FA/LDC-PVP and FA-PVP exhibited a nearly total wound closure and lowest bacterial counts by day 14 of the study. Furthermore, PLGA/PVP-based nanofibers showed limited efficacy upon daily application which requires further investigation. It is important to acknowledge that the pilot study had its limitations, namely, the inability to assess the anesthetic effect of LDC on mice and the possible presence of fungal or bacterial co-infections in the wound area. Such limitations require further investigation under more controlled experimental conditions to provide a more comprehensive understanding of the potential value of the formulated nanofibrous systems as wound dressings.

Conclusion

Wound healing is a natural physiological process that occurs in multiple intricate stages. While this process initiates a cascade of biochemical events, improper wound healing can happen in the presence of infection, which can adversely affect the structure and function of the skin in the area of injury. Existing typical wound dressings cannot provide a proper moist environment for ideal wound healing. Accordingly, the development of an antibiotic-loaded nanofibrous system can demonstrate the potential to expedite wound healing while minimizing the risk of bacterial infections. Herein, antibiotic and anesthetic drugs were successfully loaded in two fabricated nanofibrous mats using a well-established technique known as electrospinning. FA/LDC-PLGA/PVP and FA/LDC-PVP were successfully fabricated and assessed by in vitro and in vivo experiments. Characterization studies of both nanofibrous formulations showed a desirable surface morphology without beading and a high EE% of both drugs indicating successful incorporation. FA/LDC-PLGA/PVP achieved a 100% release rate of both drugs after 48 hours sustainably without any burst release, while FA/LDC-PVP released above 80% within the first 24 hours. Moreover, in vitro cell viability studies demonstrated the safety of both drugs at the selected concentration of $\leq$ 125 μg/mL which was applied in the following studies. Upon assessing for antimicrobial activity, both dual drug-loaded nanofiber systems showed potent antibacterial activity against *S. aureus*. In an infected wound model, FA/LDC-PVP and FA-PVP promoted a noticeably faster wound closure than FA/LDC-PLGA /PVP and other controls which can be indicative of their potential use against infected wounds to promote an accelerated wound healing. In conclusion, the study provided valuable insights into the therapeutic potential of dual drug-loaded electrospun nanofibrous systems in accelerating wound healing.

Data Sharing Statement

The authors confirm that the data supporting the findings of this study are available within the article.

Institutional Review Board Statement

This animal study was performed in controlled facilities in compliance with protocol number IRB 23006 approved by the Local Committee of Ethics of Research on Living Creatures in King Abdulaziz City for Science and Technology-Institutional Review Board (KACST-IRB).

Author Contributions

All authors made a significant contribution to the work reported, whether that is in the conception, study design, execution, acquisition of data, analysis and interpretation, or all these areas; took part in drafting, revising or critically

reviewing the article; gave final approval of the version to be published; have agreed on the journal to which the article has been submitted; and agree to be accountable for all aspects of the work.

Funding

This study was funded by the Innovation Challenge Competition at King Abdulaziz City for Science and Technology, Riyadh, Saudi Arabia.

Disclosure

This work was submitted to the Saudi Authority for Intellectual Property, submission number 1020243630, dated 26 June 2024. The authors declare that there are no other conflicts of interest.

References

1. McGrath JA, Eady R, Pope F. Anatomy and organization of human skin. *Rook's Textbook Dermatol*. 2004;1:3.
2. Williams A. *Transdermal and Topical Drug Delivery from Theory to Clinical Practice*. Pharmaceutical press; 2003.
3. Chereddy KK, Vandermeulen G, Préat V. PLGA based drug delivery systems: promising carriers for wound healing activity. *Wound Repair Regener*. 2016;24(2):223–236. doi:10.1111/wrr.12404
4. Braiman-Wiksman L, Solomonik I, Spira R, Tennenbaum T. Novel Insights into Wound Healing Sequence of Events. *Toxicol Pathol*. 2007;35(6):767–779. doi:10.1080/01926230701584189
5. Gurtner GC, Werner S, Barrandon Y, Longaker MT. Wound repair and regeneration. *Nature*. 2008;453(7193):314–321. doi:10.1038/nature07039
6. Zhang X, Wang Y, Gao Z, et al. Advances in wound dressing based on electrospinning nanofibers. *J Appl Polym Sci*. 2023;141(1):e54746. doi:10.1002/app.54746
7. Zhang K, Bai X, Yuan Z, et al. Layered nanofiber sponge with an improved capacity for promoting blood coagulation and wound healing. *Biomaterials*. 2019;204:70–79. doi:10.1016/j.biomaterials.2019.03.008
8. Tottoli EM, Dorati R, Genta I, Chiesa E, Pisani S, Conti B. Skin Wound Healing Process and New Emerging Technologies for Skin Wound Care and Regeneration. *Pharmaceutics*. 2020;12(8):735. doi:10.3390/pharmaceutics12080735
9. Savencu I, Iurian S, Porfire A, Bogdan C, Tomuță I. Review of advances in polymeric wound dressing films. *React Funct Polym*. 2021;168:105059. doi:10.1016/j.reactfunctpolym.2021.105059
10. Wang B, Lu G, Song K, et al. PLGA-based electrospun nanofibers loaded with dual bioactive agent loaded scaffold as a potential wound dressing material. *Colloids Surf B*. 2023;231:113570. doi:10.1016/j.colsurfb.2023.113570
11. Wang F, Hu S, Jia Q, Zhang L. Advances in Electrospinning of Natural Biomaterials for Wound Dressing. *J Nanomater*. 2020;2020(1):8719859. doi:10.1155/2020/8719859
12. Bhardwaj N, Kundu SC. Electrospinning: a fascinating fiber fabrication technique. *Biotechnol Adv*. 2010;28(3):325–347. doi:10.1016/j.biotechadv.2010.01.004
13. Juncos Bombin AD, Dunne NJ, McCarthy HO. Electrospinning of natural polymers for the production of nanofibres for wound healing applications. *Mater Sci Eng C*. 2020;114:110994. doi:10.1016/j.msec.2020.110994
14. Sun Y, Cheng S, Lu W, Wang Y, Zhang P, Yao Q. Electrospun fibers and their application in drug controlled release, biological dressings, tissue repair, and enzyme immobilization. *RSC Adv*. 2019;9(44):25712–25729. doi:10.1039/C9RA05012D
15. Li X, Wang C, Yang S, Liu P, Zhang B. Electrospun PCL/mupirocin and chitosan/lidocaine hydrochloride multifunctional double layer nanofibrous scaffolds for wound dressing applications. *Int J Nanomed*. 2018;13:5287–5299. doi:10.2147/IJN.S177256
16. Qiu H, Zhu S, Pang L, et al. ICG-loaded photodynamic chitosan/polyvinyl alcohol composite nanofibers: anti-resistant bacterial effect and improved healing of infected wounds. *Int J Pharm*. 2020;588:119797. doi:10.1016/j.ijpharm.2020.119797
17. Samadian H, Zamiri S, Ehterami A, et al. Electrospun cellulose acetate/gelatin nanofibrous wound dressing containing berberine for diabetic foot ulcer healing: in vitro and in vivo studies. *Sci Rep*. 2020;10(1):8312. doi:10.1038/s41598-020-65268-7
18. Shahriar SMS, Mondal J, Hasan MN, Revuri V, Lee DY, Lee YK. Electrospinning Nanofibers for Therapeutics Delivery. *Nanomaterials*. 2019;9(4):532. doi:10.3390/nano9040532
19. Goyal R, Macri LK, Kaplan HM, Kohn J. Nanoparticles and nanofibers for topical drug delivery. *J Control Release*. 2016;240:77–92. doi:10.1016/j.jconrel.2015.10.049
20. Jain RA. The manufacturing techniques of various drug loaded biodegradable poly(lactide-*co*-glycolide) (PLGA) devices. *Biomaterials*. 2000;21(23):2475–2490. doi:10.1016/S0142-9612(00)00115-0
21. Rahmani F, Ziyadi H, Baghali M, Luo H, Ramakrishna S. Electrospun PVP/PVA Nanofiber Mat as a Novel Potential Transdermal Drug-Delivery System for Buprenorphine: a Solution Needed for Pain Management. *Appl Sci*. 2021;11(6):2779. doi:10.3390/app11062779
22. Yu DG, Zhang XF, Shen XX, Brandford-White C, Zhu LM. Ultrafine ibuprofen-loaded polyvinylpyrrolidone fiber mats using electrospinning. *Poly Int*. 2009;58(9):1010–1013. doi:10.1002/pi.2629
23. Gilchrist SE, Lange D, Letchford K, Bach H, Fazli L, Burt HM. Fusidic acid and rifampicin co-loaded PLGA nanofibers for the prevention of orthopedic implant associated infections. *J Control Release*. 2013;170(1):64–73. doi:10.1016/j.jconrel.2013.04.012
24. Collignon P, Turnidge J. Fusidic acid in vitro activity. *Int J Antimicrob Agents*. 1999;12:S45–S58. doi:10.1016/S0924-8579(98)00073-9
25. Long J, Ji W, Zhang D, Zhu Y, Bi Y. Bioactivities and Structure–Activity Relationships of Fusidic Acid Derivatives: a Review. *Front Pharmacol*. 2021;12:759220. doi:10.3389/fphar.2021.759220
26. Alsulami KA, Bakr AA, Alshehri AA, et al. Fabrication and evaluation of ribavirin-loaded electrospun nanofibers as an antimicrobial wound dressing. *Saudi Pharm J*. 2024;32(5):102058. doi:10.1016/j.jsps.2024.102058

27. Alzahrani DA, Alsulami KA, Alsulaihem FM, et al. Dual Drug-Loaded Coaxial Nanofiber Dressings for the Treatment of Diabetic Foot Ulcer. *IJN*. 2024;19:5681–5703. doi:10.2147/IJN.S460467
28. Wayne P. *Methods for Dilution Antimicrobial Susceptibility Tests for Bacteria That Grow Aerobically*. 10th ed. Clinical and Laboratory Standards Institute CLSI; 2015.
29. Mutlu B, Çiftçi F, Üstündağ CB, Çakır-Koç R. *Lavandula stoechas* extract incorporated polylactic acid nanofibrous mats as an antibacterial and cytocompatible wound dressing. *Int J Biol Macromol*. 2023;253:126932. doi:10.1016/j.ijbiomac.2023.126932
30. Pérez M, Robres P, Moreno B, et al. Comparison of Antibacterial Activity and Wound Healing in a Superficial Abrasion Mouse Model of Staphylococcus aureus Skin Infection Using Photodynamic Therapy Based on Methylene Blue or Mupirocin or Both. *Front Med*. 2021;8:6734085. doi:10.3389/fmed.2021.673408
31. Takakura N, Sato Y, Ishibashi H, et al. A novel murine model of oral candidiasis with local symptoms characteristic of oral thrush. *Microbiol Immunol*. 2003;47(5):321–326. doi:10.1111/j.1348-0421.2003.tb03403.x
32. Williams GR, Raimi-Abraham BT, Luo CJ. *Nanofibres in Drug Delivery*. UCL press; 2018.
33. Alamer AA, Alsaleh NB, Aodah AH, et al. Development of Imeglimin Electrospun Nanofibers as a Potential Buccal Antidiabetic Therapeutic Approach. *Pharmaceutics*. 2023;15(4):1208. doi:10.3390/pharmaceutics15041208
34. Baganizi D, Nyairo E, Duncan S, Singh S, Dennis V. Interleukin-10 Conjugation to Carboxylated PVP-Coated Silver Nanoparticles for Improved Stability and Therapeutic Efficacy. *Nanomaterials*. 2017;7(7):165. doi:10.3390/nano7070165
35. Abdelkader DH, Abosalha AK, Khattab MA, Aldosari BN, Almurshedi AS. A Novel Sustained Anti-Inflammatory Effect of Atorvastatin-Calcium PLGA Nanoparticles: in vitro Optimization and In Vivo Evaluation. *Pharmaceutics*. 2021;13(10):1658. doi:10.3390/pharmaceutics13101658
36. Bastidas JG, Maurmann N, da Silveira MR, Ferreira CA, Pranke P. Development of fibrous PLGA/fibrin scaffolds as a potential skin substitute. *Biomed Mater*. 2020;15(5):055014. doi:10.1088/1748-605x/aba086
37. Marei HF, Arafa MF, Essa EA, El Maghraby GM. Lidocaine as eutectic forming drug for enhanced transdermal delivery of nonsteroidal anti-inflammatory drugs. *J Drug Delivery Sci Technol*. 2021;61:102338. doi:10.1016/j.jddst.2021.102338
38. Fan Q, Wu H, Kong Q. Superhydrophilic PLGA-Graft-PVP/PC Nanofiber Membranes for the Prevention of Epidural Adhesion. *Int J Nanomed*. 2022;17:1423–1435. doi:10.2147/IJN.S356250
39. Ahmed IS, Elnahas OS, Assar NH, Gad AM, El Hosary R. Nanocrystals of Fusidic Acid for Dual Enhancement of Dermal Delivery and Antibacterial Activity: in vitro, Ex Vivo and In Vivo Evaluation. *Pharmaceutics*. 2020;12(3):199. doi:10.3390/pharmaceutics12030199
40. Jaipakdee N, Pongjanyakul T, Limpongsa E. Preparation And Characterization Of Poly (Vinyl Alcohol)–Poly (Vinyl Pyrrolidone) Mucoadhesive Buccal Patches For Delivery Of Lidocaine Hcl. *Int J Appl Pharm*. 2018;10(1):115. doi:10.22159/ijap.2018v10i1.23208
41. Suksaeree J, Waiprib R, Pichayakorn W. Improving the Hydrophilic Properties of Deproteinized Natural Rubber Latex Films for Lidocaine Transdermal Patches by Starch Blending. *J Polym Environ*. 2021;30(4):1574–1586. doi:10.1007/s10924-021-02285-1
42. Aburayan WS, Alajmi AM, Alfahad AJ, et al. Melittin from Bee Venom Encapsulating Electrospun Fibers as a Potential Antimicrobial Wound Dressing Patches for Skin Infections. *Pharmaceutics*. 2022;14(4):725. doi:10.3390/pharmaceutics14040725
43. Alkahtani ME, Aodah AH, Abu Asab OA, Basit AW, Orlu M, Tawfik EA. Fabrication and Characterization of Fast-Dissolving Films Containing Escitalopram/Quetiapine for the Treatment of Major Depressive Disorder. *Pharmaceutics*. 2021;13(6):891. doi:10.3390/pharmaceutics13060891
44. Tawfik EA, Scarpa M, Abdelhakim HE, et al. A Potential Alternative Orodispersible Formulation to Prednisolone Sodium Phosphate Orally Disintegrating Tablets. *Pharmaceutics*. 2021;13(1):120. doi:10.3390/pharmaceutics13010120
45. Bennison LR, Miller CN, Summers RJ, Minnis AMB, Sussman G, McGuiness W. The pH of wounds during healing and infection: a descriptive literature review. *Wound Pract Res*. 2017;25(2):63–69.
46. Yoo J, Won YY. Phenomenology of the Initial Burst Release of Drugs from PLGA Microparticles. *ACS Biomater Sci Eng*. 2020;6(11):6053–6062. doi:10.1021/acsbiomaterials.0c01228
47. Kırımlıoğlu G Y. Chapter 3 - Drug loading methods and drug release mechanisms of PLGA nanoparticles. In: Kesharwani P editor. *Poly(Lactic-Co-Glycolic Acid) (PLGA) Nanoparticles for Drug Delivery*. Micro and Nano Technologies. Elsevier; 2023:55–86. doi:10.1016/B978-0-323-91215-0.00005-4.
48. Liu Y, Li C, Feng Z, Han B, Yu DG, Wang K. Advances in the Preparation of Nanofiber Dressings by Electrospinning for Promoting Diabetic Wound Healing. *Biomolecules*. 2022;12(12):1727. doi:10.3390/biom12121727
49. Jones RN, Castanheira M, Rhomberg PR, Woosley LN, Pfaller MA. Performance of Fusidic Acid (CEM-102) Susceptibility Testing Reagents: broth Microdilution, Disk Diffusion, and Etest Methods as Applied to Staphylococcus aureus. *J Clin Microbiol*. 2010;48(3):972–976. doi:10.1128/jcm.01829-09
50. Mlynarczyk-Bonikowska B, Kowalewski C, Krolak-Ulinska A, Marusza W. Molecular Mechanisms of Drug Resistance in Staphylococcus aureus. *Int J Mol Sci*. 2022;23(15):8088. doi:10.3390/ijms23158088
51. Callahan ZM, Roberts AL, Christopher AN, et al. The Effect of Commonly Used Local Anesthetic on Bacterial Growth. *J Surg Res*. 2022;274:16–22. doi:10.1016/j.jss.2021.12.040
52. Razavi BM, Fazly Bazzaz BS. A review and new insights to antimicrobial action of local anesthetics. *Eur J Clin Microbiol Infect Dis*. 2019;38(6):991–1002. doi:10.1007/s10096-018-03460-4
53. Said SS, Aloufy AK, El-Halfawy OM, Boraei NA, El-Khordagui LK. Antimicrobial PLGA ultrafine fibers: interaction with wound bacteria. *Eur J Pharm Biopharm*. 2011;79(1):108–118. doi:10.1016/j.ejpb.2011.03.002
54. De Keersmaecker SCJ, Verhoeven TLA, Desair J, Marchal K, Vanderleyden J, Nagy I. Strong antimicrobial activity of Lactobacillus rhamnosus GG against Salmonella typhimurium is due to accumulation of lactic acid. *FEMS Microbiol Lett*. 2006;259(1):89–96. doi:10.1111/j.1574-6968.2006.00250.x
55. Yi E-J, Nguyen TTM, Jin X, Bellere AD, Kim M-J, Yi T-H. Human Milk-Derived Enterococcus faecalis HM20: a Potential Alternative Agent of Antimicrobial Effect against Methicillin-Resistant Staphylococcus aureus (MRSA). *Microorganisms*. 2024;12(2):306. doi:10.3390/microorganisms12020306
56. Hameed M, Rasul A, Nazir A, et al. Moxifloxacin-loaded electrospun polymeric composite nanofibers-based wound dressing for enhanced antibacterial activity and healing efficacy. *Int J Polym Mater Polym Biomater*. 2021;70(17):1271–1279. doi:10.1080/00914037.2020.1785464